Modelling and Control of a Four-Wheel-Steering Mobile Robot

Maxim Makatchev, John J. McPhee, S. K. Tso, Sherman Y. T. Lang

Abstract— **This paper describes a dynamic model and cross-coupling control for a mobile robot with four independently steered and driven wheels. In addition to what is traditionally included in dynamic models of mobile robots, the proposed model accounts for the components of the wheel mechanisms, motors and nonlinear forces produced by the tire-ground interaction—factors affecting the ability of vehicles with redundant wheel configuration to comply with pure rolling constraints. The problem of computationally efficient control of the vehicle is solved using a low-level control loop that cross-couples steering and driving motors and is utilized in conjunction with a kinematics-based trajectory-tracking controller. The results of simulation show significant reduction of the vehicle slip due to misalignment of the wheels with moderate trajectory-tracking errors.**

Keywords— **Dynamic modelling, four-wheel steering, cross-coupling control, slippage minimization.**

I. Introduction

Research on modelling and control of wheeled vehicles can be divided into two major categories: one that is oriented towards automobiles and terrain vehicles, the other is oriented towards indoor wheeled mobile robots (WMRs). This division is based on the differences in the design of the vehicles, operational and environmental conditions. To mention a few:

- indoor WMRs usually operate within a lower speed range compared to automobiles.
- wheels of WMRs are often independently actuated, as opposed to mechanically coupled pairs of steering wheels of automobiles.
- a wheel plane of a typical WMR is normally perpendicular to the ground plane, while a wheel plane of an automobile may have a nonzero inclination angle (camber) [1], [2].

Mechanical coupling of the wheels in automobiles often allows the use of a simplified, *single-track* model for the design of motion controllers for two-wheel-steering and four-wheel-steering cars [3], [4]. Since independently actuated wheel configurations have more degrees of freedom than configurations with coupled wheels, in the modelling and control of the former it is normally desirable to explicitly account for each of the wheels of the vehicle.

Works [5], [6], and [7] are concerned with more detailed models of the four-wheel vehicles, but the controllers are still designed under the assumption that the wheels are steered in pairs. The models also utilize simplified wheel actuator dynamics that may not be appropriate for modelling of some types of WMRs, e. g. heavy vehicles with DC motor actuated wheels, for which the effects of wheel mechanism dynamics may be significant. Heavy-loading autonomous guided vehicles (AGVs) operating in manufacturing environments often belong to this class of WMRs. Independent steering and driving of the wheels of such AGVs significantly increases the class of achievable trajectories—a feature that is highly beneficial to AGV operation in congested factory or warehouse areas.

The models and controllers that explicitly deal with independent steering include kinematics-based trajectory-tracking control using dynamic feedback [8], and augmented kinematic models that account for slip due to redundancy in the configuration of the wheels [9], [10]. Arbitrary configurations of typical wheels are classified by the proposed notation of *degrees of mobility and steerability* in [11], [12]. Dynamic models are also derived, describing the relations between the configuration coordinates and the torques developed by the onboard actuators.

Despite obvious advantages that independent actuation of the wheels brings to maneuverability of a WMR, the rarely welcomed side effect is that dynamic properties of the wheel plants may easily cause deviation from the kinematic constraints of rolling with no slip (*pure rolling*) in WMRs with redundant wheel configurations (see Section II). The resulting slip contributes to dead reckoning errors and negatively affects response of the vehicle to control actions. Thus one could augment the set of conventional control objectives of such WMRs with an additional objective of minimization of slip due to dynamics of the wheel plants. This paper describes an approach to modelling and control that specifically addresses this issue.

The effect of slip due to misalignment of the wheels has been modelled via minimization of a friction functional in [9], and via least-squares estimation of the vehicle frame posture in [10]. These models, as well as those described in [11], [12], are not directly applicable for the design of the desired controller since they do not account for the source of this kind of slippage, i. e. wheel plants. Never-

This project is supported by the RGC grant 9040224 in Hong Kong and by the Strategic Research Grant 7001293 of City University of Hong Kong.

The results on the cross-coupling control were presented at the International Symposium on Robotics, Montreal, Canada, 2000.

M. Makatchev is with the Learning Research and Development Center, University of Pittsburgh, Pittsburgh, PA 15260 USA. The main body of this work was performed while he was with the Dept. of Manufacturing Engineering and Engineering Management, City University of Hong Kong, Hong Kong SAR, P. R. China (e-mail: maxim@pitt.edu).

J. J. McPhee is with the Dept. of Systems Design Engineering, University of Waterloo, Ontario, Canada N2L 3G1 (e-mail: mcphee@real.uwaterloo.ca).

S. K. Tso is with the Centre for Intelligent Design, Automation and Manufacturing, City University of Hong Kong, Hong Kong SAR, P. R. China (e-mail: mesktso@cityu.edu.hk).

S. Y. T. Lang is with the Integrated Manufacturing Technologies Institute, National Research Council of Canada, London, Ontario, Canada N6G 4X8 (e-mail: Sherman.Lang@nrc.ca).

theless, the need for deployment of the full dynamic model of the vehicle to account for the slippage can be avoided by augmenting a trajectory-based controller with a dedicated controller coordinating wheel actuators. For example, in [13] the single-track dynamic model of a four-wheel-steering vehicle is augmented by steering actuator dynamics, allowing a dedicated controller to be used for synchronization of wheel steering angles. To reduce tire slippage in the special case when steering angles are fixed, a combined controller of the driving actuators of a multiple-wheel WMR has been developed in [14]. Work [15] proposes a cross-coupling controller for a differential-drive mobile robot to reduce the robot's body orientation errors. Computational efficiency of using a kinematics-based controller for trajectory tracking augmented with the controller aimed at slippage minimization due to misalignment of the wheels has influenced our decision to follow this approach.

The controller proposed in this paper extends the coupling approach presented in [13], [14], [15] by (i) cross-coupling all four wheels of the vehicle, instead of coupling them pairwise, (ii) incorporating not only steering but also driving actuator dynamics, (iii) generalizing the control objectives so that the wheels are able to track a linear approximation of the vehicle kinematic constraints during transient states of control. This coupling scheme allows the four wheels to be steered at arbitrary angles, not necessarily the same angles as in [13].

The performance of the cross-coupling controller is evaluated (in Section IV-B) with the dynamic model developed for the AGV prototype of the project. The dynamic model of the vehicle (presented in Section III) differs from those described in [5], [6], [7] in that, in addition to nonlinear forces at the contact between the tire and the ground, it incorporates the dynamics of the components of the wheel mechanisms—significant factors affecting the errors of wheel synchronization.

II. Kinematic model

A diagram of the vehicle is presented in Figure 1. Assuming that the vehicle frame is a rigid body undergoing a planar motion, the velocities $\mathbf{v}_i$ of the wheel base points W_i are related to the velocity $\mathbf{v}_c$ of the reference point C of the frame as

$$\mathbf{v}_i = \mathbf{v}_c + \dot{\theta}\mathbf{k} \times \overrightarrow{CW_i}, \qquad i = 1, \ldots, 4, \tag{1}$$

where $\dot{\theta}$ is the angular velocity of the vehicle's frame coordinate system $\{C, x, y\}$ with respect to the fixed coordinate system of the horizontal plane $\{O, X, Y\}$, $\mathbf{k}$ is the unit vertical vector.

Pure rolling condition implies that the wheel's rotation rate $\dot{\phi}_i$ and steering angle ψ_i with respect to the frame coordinate system are such that

$$\dot{\phi}_i = \frac{|\mathbf{v}_i|}{r}, \qquad \tan\psi_i = \frac{v_{iy}}{v_{ix}}, \qquad i = 1, \ldots, 4, \tag{2}$$

where r is the radius of the wheel, v_{ix} and v_{iy} are the components of the vector $\mathbf{v}_i$ in the frame coordinate system $\{C, x, y\}$, $v_{ix} = v_{cx} - CW_{iy}\dot{\theta}$, $v_{iy} = v_{cy} + CW_{ix}\dot{\theta}$.

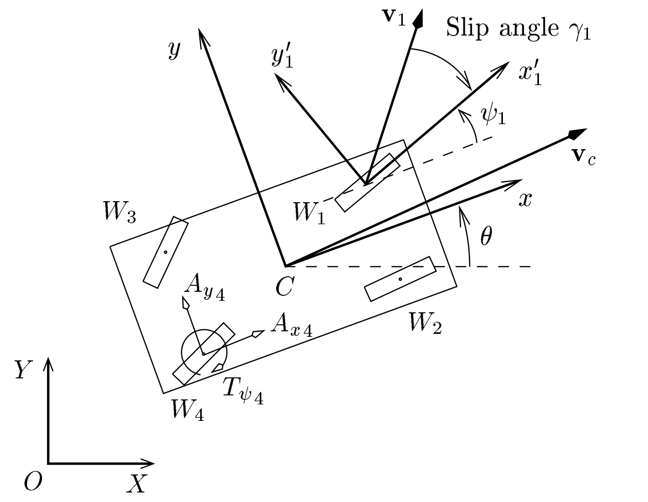

Fig. 1. Notation of kinematics of the WMR and dynamics of the frame.

The pair of equations (2) constitute the *kinematic constraint* relating driving rates and steering angles of the wheels to the linear and angular velocities of the vehicle's frame. Note that (2) implies that the slip angle of wheel i, that can be expressed as

$$\gamma_i = \cos^{-1}\left(\frac{\mathbf{v}_i \cdot \mathbf{i}'}{|\mathbf{v}_i|}\right), \tag{3}$$

should be equal to zero (thus "pure rolling"). Here the unit vector $\mathbf{i}'$ is directed along the axis x_i'.

The kinematic equation relating acceleration $\mathbf{a}_i$ of the wheel base point W_i and acceleration $\mathbf{a}_c$ of the vehicle reference point C is

$$\mathbf{a}_i = \mathbf{a}_c + \ddot{\theta}\mathbf{k} \times \overrightarrow{CW_i} - \dot{\theta}^2\overrightarrow{CW_i}. \tag{4}$$

Using the fact that $\mathbf{a}_c = (\dot{v}_x - \dot{\theta}v_y)\mathbf{i} + (\dot{v}_y + \dot{\theta}v_x)\mathbf{j}$ we have $\mathbf{a}_i = a_{x i}\mathbf{i} + a_{y i}\mathbf{j}$, where

$$a_{x i} = \dot{v}_x - \dot{\theta}v_y - CW_{ix}\dot{\theta}^2 - CW_{iy}\ddot{\theta}, \tag{5}$$

$$a_{y i} = \dot{v}_y + \dot{\theta}v_x - CW_{iy}\dot{\theta}^2 + CW_{ix}\ddot{\theta}. \tag{6}$$

III. Dynamic model

The dynamic model of the vehicle is derived by considering the dynamics of the vehicle frame, wheel struts, wheels, and wheel motors.

A. Frame dynamics

The frame longitudinal, lateral and yaw dynamic equations are:

$$ma_x = m(\dot{v}_x - \dot{\theta}v_y) = \sum_i A_{x i}, \tag{7}$$

$$ma_y = m(\dot{v}_y + \dot{\theta}v_x) = \sum_i A_{y i}, \tag{8}$$

$$I\ddot{\theta} = \sum_i P_i \tag{9}$$

respectively, where A_{xi} and A_{yi} are the x-component and the y-component of reaction at the steer joint W_i, $P_i = -T_{\psi i} + CW_{ix}A_{yi} - CW_{iy}A_{xi}$ is the vertical component of the total torque applied to the frame via the steer joint W_i, $T_{\psi i}$ is the torque applied to the wheel strut by the steering DC motor.

We neglect the change of horizontal components P_{xi}, P_{yi} of the torque applied to the vehicle frame via the steer joint, assuming that the normal reactions at the wheel-ground contact points are equal for all wheels and remain constant.

B. Wheel strut dynamics

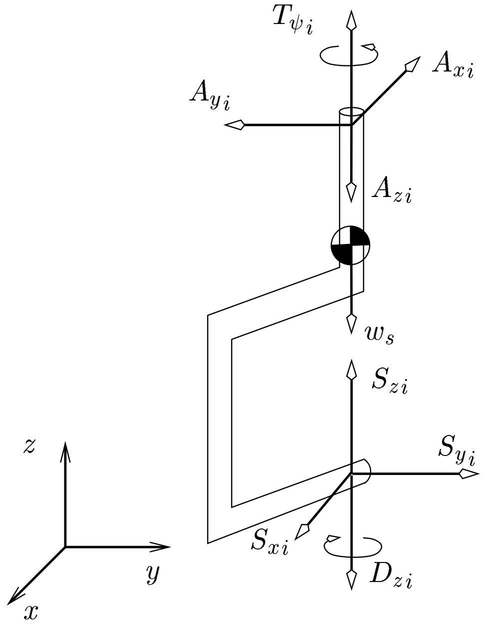

Fig. 2. Dynamics of the wheel strut.

We assume that for each wheel i the gravity centers of the strut and the wheel, the point of the wheel contact with the ground, geometric center of the wheel, and steer joint W_i are all on a single vertical line. As with the frame, we neglect the horizontal components of the total moment of the wheel strut:

$$\begin{aligned} m_s a_{xi} &= S_{xi} - A_{xi}, && (10)\\ m_s a_{yi} &= S_{yi} - A_{yi}, && (11)\\ w_s &= S_{zi} - A_{zi}, && (12)\\ I_s(\ddot{\theta} + \ddot{\psi}_i) &= T_{\psi i} - D_{zi}, && (13) \end{aligned}$$

where w_s is the weight of the wheel strut, I_s is its moment of inertia around the vertical axis, S_i and D_i is the reaction force and torque at the wheel-strut revolute joint respectively (Fig. 2).

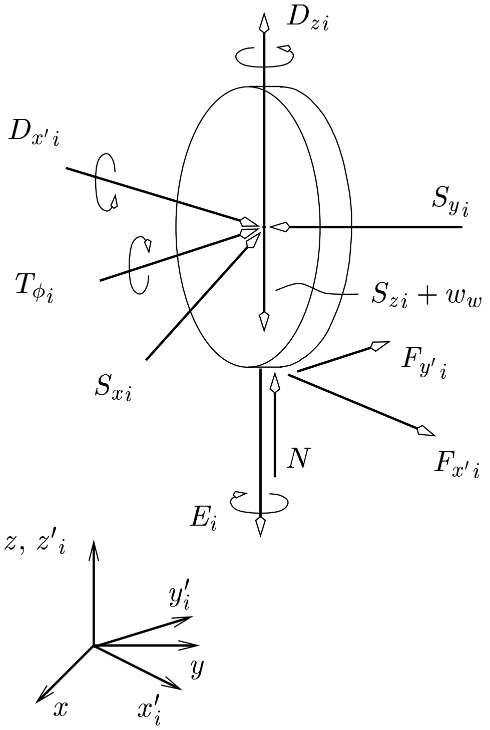

Fig. 3. Dynamics of the wheel.

C. Wheel dynamics

The forces applied to the wheel are related as follows:

$$\begin{aligned} m_w a_{xi} &= F_{xi} - S_{xi}, && (14)\\ m_w a_{yi} &= F_{yi} - S_{yi}, && (15)\\ w_w &= N - S_{zi}, && (16) \end{aligned}$$

where F_i is the tire contact force and N is the normal force at the point of the tire-ground contact, w_w is the weight of the wheel.

The total moment produced by couples and forces applied to wheel i is

$$\begin{aligned} \mathbf{M}_i &= \mathbf{T}_{\phi i} + \mathbf{D}_{zi} - \mathbf{E}_i + \mathbf{D}_{x'i} - r\mathbf{k}' \times (F_{x'i}\mathbf{i}' + F_{y'i}\mathbf{j}') \\ &= (D_{x'i} + rF_{y'i})\mathbf{i}' + (T_{\phi i} - rF_{x'i})\mathbf{j}' + (D_{zi} - E_i)\mathbf{k}', \end{aligned} \quad (17)$$

where E_i is the magnitude of the aligning torque $\mathbf{E}_i$ due to friction at the point of the tire-ground contact.

We assume the wheel to be cylindrical so that the axes x'_i, y'_i, z'_i are its principal axes of inertia. The dynamic equations for the wheel i are:

$$\begin{aligned} M_{xi} &= I_{x'x'}\dot{\omega}_{x'i} + (I_{z'z'} - I_{y'y'})\omega_{y'i}\omega_{z'i}, && (18)\\ M_{yi} &= I_{y'y'}\dot{\omega}_{y'i} + (I_{x'x'} - I_{z'z'})\omega_{x'i}\omega_{z'i}, && (19)\\ M_{zi} &= I_{z'z'}\dot{\omega}_{z'i} + (I_{y'y'} - I_{x'x'})\omega_{x'i}\omega_{y'i}, && (20) \end{aligned}$$

where $I_{x'x'} = I_{z'z'} = I_t$ is the transverse moment of inertia and $I_{y'y'} = I_a$ is the axial moment of inertia of the wheel. Assuming that the x'_i-component of the angular velocity of the wheel is zero (no camber), the angular velocity of the wheel i is

$$\boldsymbol{\omega}_i = (\dot{\theta} + \dot{\psi}_i)\mathbf{k}' + \dot{\phi}_i\mathbf{j}'. \quad (21)$$

Substitution of (21) into (18)–(20) and using (17) and (13) gives us the expressions for the steering and driving torques respectively:

$$T_{\psi_i} = (I_s + I_t)(\ddot{\theta} + \ddot{\psi}_i) + E_i, \tag{22}$$

$$T_{\phi_i} = I_a \ddot{\phi}_i + r F_{x'i}. \tag{23}$$

D. Dynamics of wheel motors

Assuming that the ratio of armature-winding inductance to resistance of the motors is small, the equations governing the dynamics of the (i) steering and (ii) driving motors of the wheel i are as follows:
(i) steering motors

$$k_1' e_{\psi_i} = k_3' \dot{\psi}_i + R' i_{\psi_i}, \tag{24}$$

$$k_2' i_{\psi_i} = (I_s + I_t)(\ddot{\theta} + \ddot{\psi}_i) + b' \dot{\psi}_i + E_i, \tag{25}$$

where $(I_s + I_t)(\ddot{\theta} + \ddot{\psi}_i) + E_i = T_{\psi_i}$ is the steering torque applied to the wheel strut, i_{ψ_i} is the armature current and e_{ψ_i} is the input voltage of the motor, and $b'\dot{\psi}_i$ is the energy loss due to the friction in the motor and in the gear train;
(ii) driving motors

$$k_1'' e_{\phi_i} = k_3'' \dot{\phi}_i + R'' i_{\phi_i}, \tag{26}$$

$$k_2'' i_{\phi_i} = I_a \ddot{\phi}_i + b'' \dot{\phi}_i + r F_{x'i}, \tag{27}$$

where $I_a \ddot{\phi}_i + r F_{x'i} = T_{\phi_i}$ is the driving torque applied to the wheel, i_{ϕ_i} is the armature current and e_{ϕ_i} is the input voltage of the motor, and $b''\dot{\phi}_i$ is the energy loss due to the friction in the motor and in the gear train.

E. Tire-ground contact

Although the the lateral (cornering) and longitudinal (tractive) tire friction forces $F_{y'i}$ and $F_{x'i}$ are modelled in a nonlinear fashion similar to the one suggested in [1] and [2], a number of modifications is done for the simulation of the particular AGV for the sake of simplicity and computational efficiency of the model. The cornering force on the tire is set to reach its maximum magnitude μN for the absolute values of the slip angle greater than the critical value γ_{cr}, and is approximated by the linear function $F_{y'i} = -\mu N \gamma_i / \gamma_{cr}$ for the subcritical values of the slip angle. Similarly the magnitude of the tractive force is limited by μN for the absolute values of the longitudinal slip greater than Δ_{cr}, where the longitudinal slip is defined as $\Delta_i = \mathbf{v}_i \cdot \mathbf{i}' - \dot{\phi}_i r$. For the subcritical values of the longitudinal slip the tractive force is approximated as $F_{x'i} = -\mu N \Delta_i / \Delta_{cr}$. Note that for the sake of simplicity and taking into account the relatively narrow range of the velocities of the AGV prototype as opposed to automobiles, the longitudinal slip is defined as pure difference between the respective velocities, without involvement of the ratio as in [1],[2]. Mutual effects between the cornering and tractive forces are neglected.

Provided that the steering rates are relatively small compared to the respective driving rates, the aligning torque due to friction E_i can be assumed to be much smaller than its maximum possible value and therefore is neglected in the following simulation.

F. Vehicle Dynamics

Combining (7)–(9), (10)–(13), (14), (15), (5), (6) with (24)–(27), (22), (23), the state-space model of the vehicle can be presented as:

$$\begin{bmatrix} \dot{v}_x \\ \dot{v}_y \\ \ddot{\theta} \\ \ddot{\psi}_{1-4} \\ \ddot{\phi}_{1-4} \end{bmatrix} = \begin{array}{l} \mathbf{M}^{-1}\mathbf{Q}(v_x, v_y, \dot{\theta}, \dot{\psi}_{1-4}, \dot{\phi}_{1-4}, \\ \quad \psi_{1-4}, \phi_{1-4}, e_{\psi_{1-4}}, e_{\phi_{1-4}}), \end{array} \tag{28}$$

where matrices $\mathbf{M}$ and $\mathbf{Q}$ are specified in the Appendix.

IV. Control

A. Cross-coupling controller

The kinematics-based trajectory-tracking control via *linearizing dynamic feedback* [8] is an efficient solution for the problem of the WMR frame posture control. Given the state vector of the vehicle frame and the reference trajectory, the controller output is the desired state vector for the next time instance. Using the components of this state vector that correspond to the desired linear and angular velocities of the frame ($\mathbf{v}_c$ and $\dot{\theta}$ respectively) and pure rolling condition from Section II we can obtain the desired values of wheel plants $\dot{\phi}_{id}$, ψ_{id}. Unfortunately, even if at the previous time instance wheel actuators complied with the pure rolling condition, independent transient errors during the control of the actuators towards the next set of desired values are likely to result in the failure to comply with the pure rolling condition. To preserve the computational feasibility of the kinematics-based control and to account for tire slip due to misalignment of the wheels, we propose to augment the kinematics-based trajectory-tracking controller with a cross-coupling controller of the wheel actuators.

The proposed cross-coupling controller is based on the idea of a piecewise linear approximation of the trajectory corresponding to states satisfying the pure rolling condition in the space of steering angles and driving rates. One such approximation between the points corresponding to the initial and desired states, when projected on the subspace corresponding to two steering angles can be represented by the constraint

$$\frac{\psi_i - \psi_{id}}{\delta_i} = \frac{\psi_j - \psi_{jd}}{\delta_j}, \tag{29}$$

$$\delta_i = \psi_{is} - \psi_{id} \neq 0, \quad \delta_j = \psi_{js} - \psi_{jd} \neq 0, \tag{30}$$

where ψ_{is}, ψ_{js} are initial and ψ_{id}, ψ_{jd} are desired steering angles, all satisfying pure rolling condition. For example, in Figure 6(a), the o-marked line corresponds to the trajectory in the subspace of two steering angles satisfying pure rolling condition, and the linear approximation between initial ($\psi_{1s} = \psi_{2d} = 0°$), and desired ($\psi_{1d} = 38.8°$,

$\psi_{2d} = 20.1°$) states would be a straight-line segment connecting them. We refer to (29), (30) as *the condition of proportional errors* between the steering actuators i and j.

The respective projection on the subspace of a driving rate and the steering angle can be represented by the constraint

$$\frac{\dot{\phi}_i - \dot{\phi}_{id}}{\varepsilon_i} = \frac{\psi_j - \psi_{jd}}{\delta_j}, \tag{31}$$

$$\varepsilon_i = \dot{\phi}_{is} - \dot{\phi}_{id} \neq 0, \quad \delta_j = \psi_{js} - \psi_{jd} \neq 0, \tag{32}$$

where $\dot{\phi}_{is}$ is initial and $\dot{\phi}_{id}$ is desired driving rate of the driving actuator i, ψ_{is} and ψ_{id} same as above, all satisfying the pure rolling condition.

The constraint corresponding to the condition of proportional errors between two driving actuators can be formulated in a similar fashion. The condition of proportional errors induces a binary relation R in the set of controlled variables $\{a_1 = \psi_1, \ldots, a_4 = \psi_4, a_5 = \dot{\phi}_1, \ldots, a_8 = \dot{\phi}_8\}$. Due to the fact that the relation R is symmetric and transitive, the condition that the graph with vertices from $\{a_1, \ldots, a_8\}$ and edges corresponding to pairs $(a_i, a_j) \in R$ is a connected graph is sufficient to guarantee that every pair of variables is in R (the graph is complete). The trajectory corresponding to the linear approximation between the initial and desired states in the space of controlled variables $\{a_1, \ldots, a_8\}$ can be produced by (1) satisfying the condition of proportional errors on the whole set (or a sufficient subset, in the sense described above) of all pairs of variables while (2) controlling one of the variables from its initial to its desired value.

Let the discrete-time state-space model of the steering actuator i be

$$\begin{bmatrix} x_{2i-1}(k+1) \\ x_{2i}(k+1) \end{bmatrix} = \mathbf{G_i} \begin{bmatrix} x_{2i-1}(k) \\ x_{2i}(k) \end{bmatrix} + \mathbf{H_i} u_i(k),$$

where $x_{2i-1}(k)$ is equal to the steering angle ψ_i at the step k, so that $x_1(k) = \psi_1, \ldots, x_7(k) = \psi_4$, $x_{2i}(k)$ is an appropriate state variable depending on the method of discretization, the plant input $u_i(k)$ is equal to I_i at the step k, $\mathbf{G_i}$ is the state matrix, and $\mathbf{H_i}$ is the input matrix.

The discrete-time state-space model of the vehicle steering system can be represented by

$$\begin{aligned} \mathbf{x}(k+1) &= \mathbf{G}\mathbf{x}(k) + \mathbf{H}\mathbf{u}(k), \\ \mathbf{y}(k) &= \mathbf{C}\mathbf{x}(k), \end{aligned} \tag{33}$$

with the state vector $\mathbf{x} = [x_1\ x_2\ x_3\ x_4\ x_5\ x_6\ x_7\ x_8]^T$, and the control inputs $\mathbf{u} = [I_1\ I_2\ I_3\ I_4]^T$, and

$$\mathbf{G} = \begin{bmatrix} \mathbf{G_1} & \mathbf{0} & \mathbf{0} & \mathbf{0} \\ \mathbf{0} & \mathbf{G_2} & \mathbf{0} & \mathbf{0} \\ \mathbf{0} & \mathbf{0} & \mathbf{G_3} & \mathbf{0} \\ \mathbf{0} & \mathbf{0} & \mathbf{0} & \mathbf{G_4} \end{bmatrix},$$

$$\mathbf{H} = \begin{bmatrix} \mathbf{H_1} & \mathbf{0} & \mathbf{0} & \mathbf{0} \\ \mathbf{0} & \mathbf{H_2} & \mathbf{0} & \mathbf{0} \\ \mathbf{0} & \mathbf{0} & \mathbf{H_3} & \mathbf{0} \\ \mathbf{0} & \mathbf{0} & \mathbf{0} & \mathbf{H_4} \end{bmatrix}.$$

The output matrix and the reference value

$$\mathbf{C} = \begin{bmatrix} 1 & 0 & 0 & 0 & 0 & 0 & 0 & 0 \\ \frac{1}{\delta_1} & 0 & -\frac{1}{\delta_2} & 0 & 0 & 0 & 0 & 0 \\ \frac{1}{\delta_1} & 0 & 0 & 0 & -\frac{1}{\delta_3} & 0 & 0 & 0 \\ \frac{1}{\delta_1} & 0 & 0 & 0 & 0 & 0 & -\frac{1}{\delta_4} & 0 \end{bmatrix}, \tag{34}$$

$$\mathbf{y_d} = \begin{bmatrix} \psi_{1d} \\ \frac{\psi_{1d}}{\delta_1} - \frac{\psi_{2d}}{\delta_2} \\ \frac{\psi_{1d}}{\delta_1} - \frac{\psi_{3d}}{\delta_3} \\ \frac{\psi_{1d}}{\delta_1} - \frac{\psi_{4d}}{\delta_4} \end{bmatrix} \tag{35}$$

implement the condition of proportional errors for the system (33), so that the steering actuator errors of wheels 2, 3 and 4 are kept proportional to the steering actuator error of wheel 1.

Similarly to [13], we treat the cross-coupling problem as a regulation problem and apply linear quadratic optimal regulator (LQR) theory for the controller design [16].

As this study is primarily concerned with the cross-coupling of the steering actuators, we assume that the driving actuators have fast enough response so that they can effectively track the reference inputs that are directly fed from the respective steering actuator control loops. Driving actuator reference inputs

$$\dot{\phi}_{ir} = \dot{\phi}_{is} + \frac{\varepsilon_i}{\delta_i}\left(\psi_i - \psi_{is}\right) \tag{36}$$

implement the condition of proportional errors between the steering actuator and the driving actuator of the wheel i.

The steering component of the control architecture is illustrated in Figure 4.

B. Simulation results

Simulation studies have been carried out with the dynamic model of the vehicle implemented in Matlab. We compare the performance of three schemes of wheel actuator coupling in the experiments with the turning maneuver.

The reference trajectory consists of a straight-line interval and a circular arc of the radius $R = 2$ m with the center located towards the side of the vehicle corresponding to the wheels 1 and 3. The reference frame linear velocity is 0.6 m/s, the reference yaw angle is equal to the reference path slope angle at every instant. Given these settings and constraints (1), (2) during the line-interval following all reference steering angles are equal to zero, and during the circular-arc following the reference steering angles are obtained by direct computation as $\psi_{1d} = -\psi_{3d} = 38.8°$, $\psi_{2d} = -\psi_{4d} = 20.1°$.

Some of the measurements of the modelled AGV prototype are as follows: $|CW_{ix}| = 1$ m, $|CW_{iy}| = 0.75$ m, $r = 0.12$ m, mass of the frame $m = 300$ kg, moment of inertia of the frame $I = 400$ kg·m^2. To avoid the necessity of the plant estimation modules, the parameters of the wheel plants are set to have known constant values as follows:

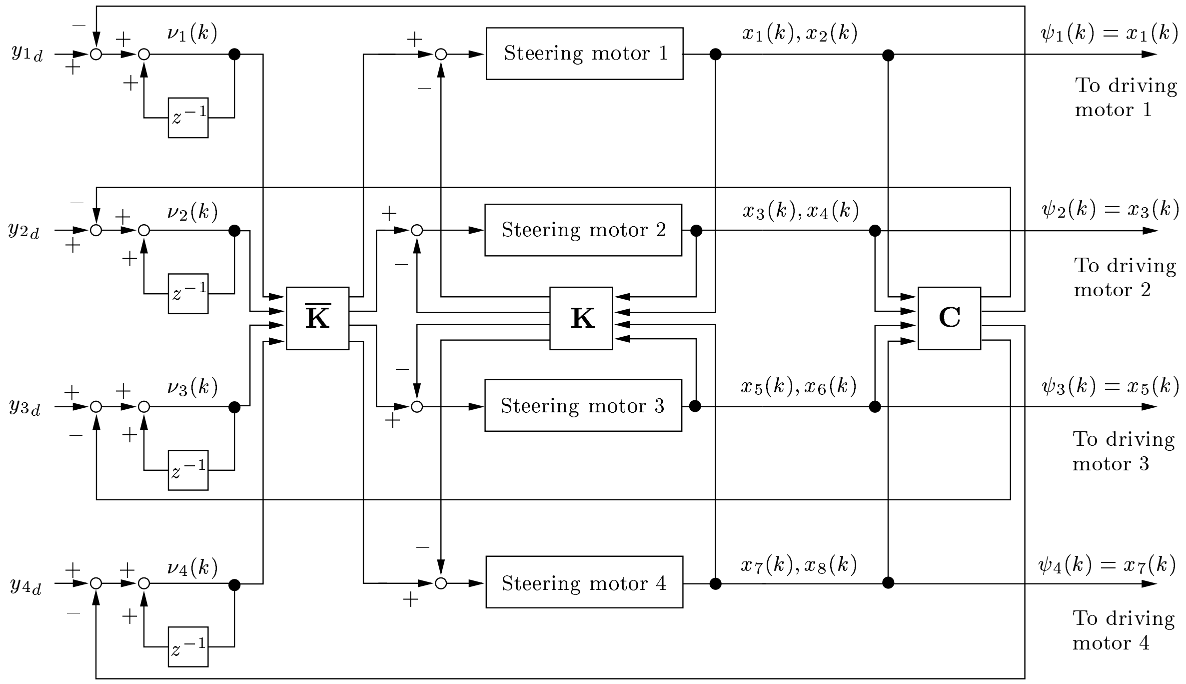

Fig. 4. Cross-coupling control system (block z^{-1} represents the discrete-time integrator).

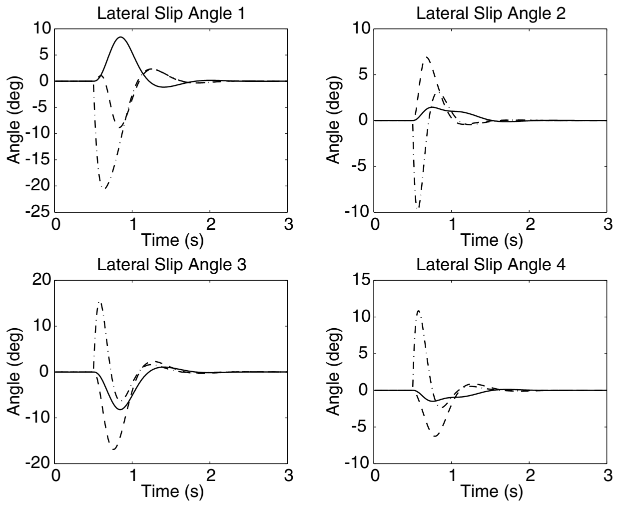

(a) Lateral slip angles.

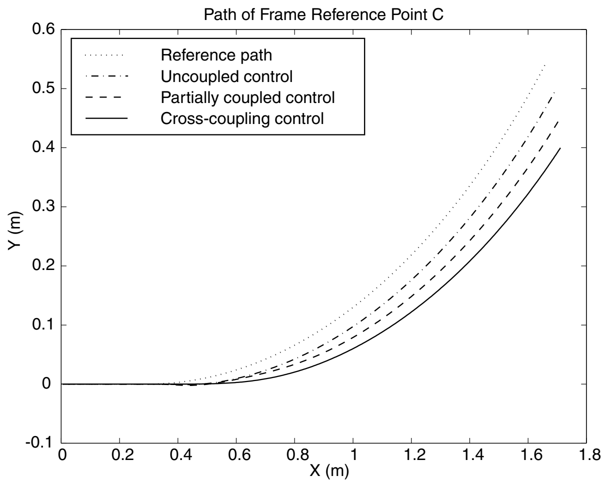

(b) Path of frame reference point.

Fig. 5. Performance of the different control schemes: dash-dotted line—uncoupled control; dashed line—partially coupled control (uncoupled controller for the steering motors, with the driving motors coupled with the respective steering motors); solid line—cross-coupling control of the steering and driving motors.

$$\mathbf{G_1} = \begin{bmatrix} 1.968 & 1 \\ -0.9675 & 0 \end{bmatrix}, \quad \mathbf{H_1} = \begin{bmatrix} 0.0001533 \\ 0.0001516 \end{bmatrix},$$

$$\mathbf{G_2} = \begin{bmatrix} 1.785 & 1 \\ -0.7851 & 0 \end{bmatrix}, \quad \mathbf{H_2} = \begin{bmatrix} 0.001751 \\ 0.001615 \end{bmatrix},$$

$$\mathbf{G_3} = \begin{bmatrix} 1.802 & 1 \\ -0.8017 & 0 \end{bmatrix}, \quad \mathbf{H_3} = \begin{bmatrix} 0.001605 \\ 0.001491 \end{bmatrix},$$

$$\mathbf{G_4} = \begin{bmatrix} 1.768 & 1 \\ -0.768 & 0 \end{bmatrix}, \quad \mathbf{H_4} = \begin{bmatrix} 0.00184 \\ 0.001685 \end{bmatrix},$$

sampling time is 0.01 s. The parameters related to the forces at the point of the tire-ground contact are $\mu = 0.8$, $\gamma_{cr} = 4°, \Delta_{cr} = 0.05$ m/s. The values of other relevant parameters of the model can be found in [16], [17].

Three cross-coupling schemes are tested: uncoupled control; partially coupled control (uncoupled control of the steering motors with the driving motors coupled with the respective steering motors according to (36)); cross-coupling control (LQR-based controller for the steering motors that corresponds to (34), (35), with the driving motors coupled with the respective steering motors according to (36)). Results of the simulation are shown in Figure 5. The simulated and the ideal (pure rolling) trajectory in the space of two steering angles are shown in Figure 6.

The path-following error is larger for the coupling controllers (Fig. 5(b)) since the "fast" wheel actuators are slowed down to synchronize with the "slow" ones. The maximum lateral slip angles are at least two times smaller ($8°$ and $-7°$ under cross-coupling as compared to $-21°$ and $16°$ without cross-coupling) for the inner steering wheels (wheels 1 and 3) that are subject to the most severe slippage conditions (Fig. 5(a)).

V. Conclusions

We study the problem of slippage due to misalignment of the wheels of a four-wheel-steering mobile robot and its solution via tracking of the linear approximation of the kinematic constraints during transient states of control. This approach allows for design of the computationally efficient LQR controller that cross-couples steering and driving actuators. The results of the simulation performed with the dynamic model of the vehicle show significant reduction of the lateral slip angles at the expense of increased trajectory tracking errors.

It remains to be investigated how the proposed controller (augmented with the wheel plant estimators) performs with the vehicle prototype. Some applications may desire control over the trade-off between precision of trajectory-tracking and slippage. Sensitivity of this trade-off to the parameters of the cross-coupling controller is also a problem for further investigation.

Acknowledgments

The authors would like to acknowledge the assistance of staff of CIDAM, City University of Hong Kong, in particular Eric Fung and Nigel Lee. We also thank Michael Cotsaftis for helpful discussions and comments.

Appendix

I. Nomenclature

reaction force and torque at steer joint	A_i, T_{ψ_i}
mass and moment of inertia of the frame	m, I
reaction force and torque at wheel-strut joint	S_i, D_i
mass and weight of the strut	m_s, w_s
moment of inertia of the strut	I_s
lateral tire friction (cornering) force	$F_{y'i}$
longitudinal tire friction (tractive) force	$F_{x'i}$
normal force at the tire-ground contact	N
tire-ground friction coefficient	μ
aligning torque due to friction	E_i
steering torque	T_{ψ_i}
driving torque	T_{ϕ_i}
mass and weight of the wheel	m_w, w_w
radius of the wheel	r
input voltage of the motors	e_{ψ_i}, e_{ϕ_i}
amplifier constants	k_1', k_1''
motor torque constants	k_2', k_2''
back emf constants of the motors	k_3', k_3''
armature current of the motors	i_{ψ_i}, i_{ϕ_i}
resistance of the motors	R', R''
viscous-friction coefficients	b', b''

II. Generalized mass and force matrices

The elements of the matrix of generalized masses $\mathbf{M_{5\times5}}$ are as follows:

$$\begin{aligned}
M_{1,1} &= M_{2,2} = m + \sum_i (m_s + m_w), \\
M_{1,3} &= M_{3,1} = -\sum_i (m_s + m_w) CW_{iy}, \\
M_{2,3} &= M_{3,2} = \sum_i (m_s + m_w) CW_{ix}, \\
M_{3,3} &= I + \sum_i (m_s + m_w) {CW_i}^2, \\
M_{4,3} &= M_{4,4} = I_s + I_t, \quad M_{5,5} = I_a,
\end{aligned}$$

and the rest of elements are zeros. The elements of the vector of generalized forces $\mathbf{Q_{5\times1}}$ are as follows:

$$\begin{aligned}
Q_{1,1} &= m v_y \dot\theta \\
&\quad + \sum_i \left(F_{xi} + (m_s + m_w) \left(v_y \dot\theta + CW_{ix} \dot\theta^2 \right) \right), \\
Q_{2,1} &= -m v_x \dot\theta \\
&\quad + \sum_i \left(F_{y_i} - (m_s + m_w) \left(v_x \dot\theta + CW_{iy} \dot\theta^2 \right) \right), \\
Q_{3,1} &= -\sum_i \left(T_{\psi_i} + \left(CW_{ix} F_{y_i} - CW_{iy} F_{xi} \right) \right. \\
&\quad \left. - \dot\theta \left(m_s + m_w \right) \left(CW_{ix} v_x + CW_{iy} v_y \right) \right), \\
Q_{4,1} &= T_{\psi_i} - E_i, \quad Q_{5,1} = T_{\phi_i} - r F_{x'i},
\end{aligned}$$

where steering and driving torques are derived from (24)–(27) with the armature voltage e_ψ, e_ϕ of the steering and driving motors given.

References

[1] T. D. Gillespie, *Fundamentals of Vehicle Dynamics*, Society of Automotive Engineers, 1992.

[2] J. Y. Wong, *Theory of Ground Vehicles*, Wiley, New York, 1993.

[3] J. Ackermann, "Robust decoupling, ideal steering dynamics and yaw stabilization of 4ws cars," *Automatica*, vol. 30, no. 11, pp. 1761–1768, 1994.

[4] A. Y. Lee, "A preview steering autopilot control algorithm for four-wheel-steering passenger vehicles," *Journal of Dynamic Systems, Measurement, and Control*, vol. 114, pp. 401–408, September 1992.

[5] W. Langson and A. Alleyne, "Multivariable bilinear vehicle control using steering and individual wheel torques," *Journal of Dynamic Systems, Measurement and Control*, vol. 121, pp. 631–637, December 1999.

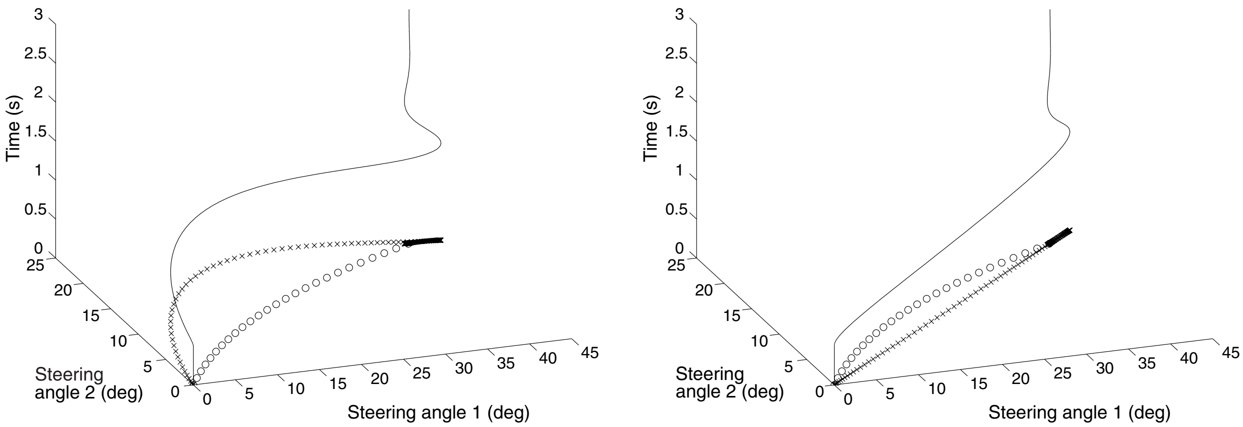

(a) Uncoupled control.

(b) Coupled control.

Fig. 6. Steering angles of wheels 1 and 2 under different control schemes. For each subfigure the solid line corresponds to the actual steering angles of the wheels, the x-marked line is the projection of the 3D trajectory represented by the solid line on the 2D space of steering angles (without time), and the o-marked line is the trajectory in the space of steering angles that corresponds to the no-slip steering.

[6] N. Matsumoto and M. Tomizuka, "Vehicle lateral velocity and yaw rate control with two independent control inputs," *Trans. of the ASME*, vol. 114, pp. 606–613, December 1992.

[7] S.-H. Yu and J. J. Moskwa, "A global approach to vehicle control: coordination of four wheel steering and wheel torques," *Journal of Dynamic Systems, Measurement and Control*, vol. 116, pp. 659–667, December 1994.

[8] B. Thuilot, B. d'Andréa Novel, and A. Micaeli, "Modeling and feedback control of mobile robots equipped with several steering wheels," *IEEE Trans. on Robotics and Automation*, vol. 12, no. 3, pp. 375–390, June 1996.

[9] J. C. Alexander and J. H. Maddocks, "On the kinematics of wheeled mobile robots," *International Journal of Robotics Research*, vol. 8, no. 5, pp. 15–27, 1989.

[10] T. Burke and H. F. Durrant-Whyte, "Kinematics for modular wheeled mobile robots," in *Proc. of the 1993 IEEE/RSJ Int. Conf. on Intelligent Robots and Systems*, Yokohama, Japan, 1993.

[11] G. Campion, G.Bastin, and B. d'Andréa Novel, "Structural properties and classification of kinematic and dynamic models of wheeled mobile robots," *IEEE Trans. on Robotics and Automation*, vol. 12, pp. 47–62, 1996.

[12] C. Canudas de Wit, B. Siciliano, and G. Bastin, Eds., *Theory of Robot Control*, chapter 7, Springer, 1996.

[13] N. Matsumoto, H. Kuraoka, and M. Ohba, "An experimental study on vehicle lateral and yaw motion control," in *Proc. of Int. Conf. on Industrial Electronics, Control and Instrumentation (IECON)*, 1991, vol. 1, pp. 113–118.

[14] D. B. Reister and M. A. Urensen, "Position and constraint force control of a vehicle with two or more steerable drive wheels," *IEEE Trans. on Robotics and Automation*, vol. 9, no. 6, pp. 723–731, 1993.

[15] L. Feng, Y. Koren, and J. Borenstein, "Cross-coupling motion controller for mobile robots," *IEEE Control Systems Magazine*, pp. 35–43, December 1993.

[16] M. Makatchev, S. Y. T. Lang, S. K. Tso, and J. J. McPhee, "Cross-coupling control for slippage minimization of a four-wheel-steering mobile robot," in *Proc. of the 31st Int. Symposium on Robotics (ISR'2000)*, Montreal, Canada, May 2000, pp. 42–47.

[17] M. Makatchev, "Computational issues on design and implementation of an autonomous guided vehicle," M.Phil. thesis, City University of Hong Kong, 2001.

Maxim Makatchev received his Diploma in applied mathematics from Lomonosov Moscow State University in 1997 and M.Phil. degree in mechatronic engineering from City University of Hong Kong in 2001. His main research interests are algorithms and complexity, particularly in robotics, artificial intelligence and logic. He is currently with the Learning Research and Development Center at the University of Pittsburgh, working on knowledge representation and automated reasoning in the domain of qualitative physics.

John McPhee received his PhD in mechanical engineering in 1990, and joined Systems Design Engineering at the University of Waterloo in 1992. His main area of research is the dynamic modelling and simulation of multibody mechatronic systems, with particular focus on robots and vehicles. He is an Advisory Editor for the journal Multibody System Dynamics, and an Associate Editor for Mechanics of Structures and Machines. He received a Premier's Research Excellence Award in 2000, and the I. W. Smith award in 2001 from the Canadian Society of Mechanical Engineers for "outstanding contributions to creative mechanical engineering."

Professor S. K. Tso obtained his BSc(Eng) and PhD degree from the University of Hong Kong and University of Birmingham, UK, respectively, in electrical and electronic engineering. He has carried out research in the broad field of industrial electronics, automation and control. He is Professor of Mechatronics and Automation in the City University of Hong Kong, and director of the Consortium of Intelligent Design, Automation and Mechatronics (CIDAM). He has held visiting professorships in many universities and served as external examiners in a number of universities. His CIDAM team is the 2002 recipient of a CMA Award for their service robotics contribution in Hong Kong.

Dr. Sherman Lang is a native of Victoria, B. C., Canada. He obtained B.A.Sc., M.A.Sc. and Ph.D. degrees in Systems Design Engineering from the University of Waterloo. Dr. Lang has held positions with the Laboratory for Biomedical Engineering of the Medical Engineering Section of the Division of Electrical Engineering of the National Research Council of Canada, the Autonomous Systems Laboratory of the Institute for Information Technology of the National Research Council of Canada, and the Department of Manufacturing Engineering and Engineering Management of the City University of Hong Kong. He is currently with the Integrated Manufacturing Technologies Institute of the National Research Council of Canada. His research interests include mobile robots, autonomous guided vehicles, mechatronic systems, vision and sensor systems, intelligent production systems and integrated design systems.